Macromolecules

ARTICLE

pubs.acs.org/Macromolecules

# Formation of a Liquid-Crystalline Interpenetrating Poly(ionic liquid) Network Hydrogel

Gregory A. Becht,[†] Marina Sofos,[†] Sönke Seifert,[‡] and Millicent A. Firestone*[,†]

[†]Materials Science and [‡]X-ray Sciences Divisions, Argonne National Laboratory, 9700 South Cass Avenue, Argonne, Illinois 60439, United States

Supporting Information

**ABSTRACT:** Preparation of a liquid-crystalline ionic-liquid (IL)-based interpenetrating polymer network (IPN) is described. The IPN is prepared sequentially by first photopolymerizing a self-assembled aqueous mixture of an IL monomer (1-(10-(acryloyloxy)decyl)-3-methylimidazolium chloride) that possesses an acryloyl moiety at the terminus of a $C_{10}$ alkyl chain of the IL cation. In the second step, an acrylate counteranion is introduced and then photopolymerized to yield a durable self-supporting network polymer. Thermal analysis indicates the formation of a homogeneous (well-blended constituent polymers) IPN. The IPN adopts a lamellar structure possessing some residual in-plane tetragonal perforations, as evidenced by small-angle X-ray scattering (SAXS). The IPN can absorb large quantities of water, swelling to nearly 60 times its original volume, but retains mechanical integrity making it a durable hydrogel.

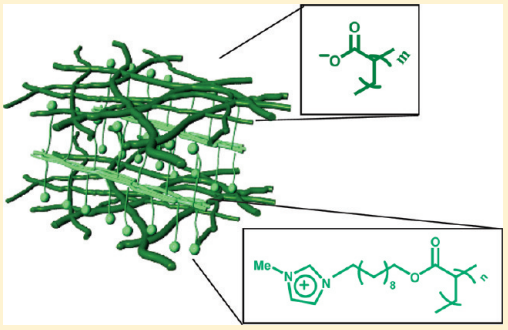

## INTRODUCTION

Interpenetrating polymer networks (IPNs) consist of two distinct polymer components which are interlaced on a molecular length scale and resist separation due to noncovalent physical entanglement.[1,2] IPNs can be prepared by reaction of the constituents simultaneously or sequentially. Sequential IPNs can be formed by first swelling a network polymer after which a second monomer is introduced and polymerized. Ideally, the entanglement of the two networks should ensure good miscibility of the two components and promote enhanced dimensional stability. Thus, a major motivator for formation of IPNs is to improve the mechanical properties of polymers.

There is increased interest in the polymeric forms of ionic liquids (poly(IL)s) and their potential as a new class of materials that combine the novel properties of ILs with improved mechanical durability and dimensional control (i.e., molecular architecture) resulting from polymerization.[3−10] Imidazolium-based poly(IL)s, which have been shown to form liquid-crystalline phases, can be prepared employing several approaches including using either a polymerizable cation or anion to generate a macromolecular polyelectrolyte.[4] For example, polymerization of the IL cation can be readily achieved through introduction of either an acryloyl or vinyl group.[11,12] Acryloyl-containing imidazolium-based IL monomers (ILMs) have been reported and shown to be readily photopolymerized into nanostructured hydrogels.[13,14] The poly(IL)s swell dramatically in water to produce a material with diminished mechanical integrity.[13] Alternatively, polymerization and cross-linking of the counteranion have also been demonstrated.[15,16] A polymerizable acrylate anion can be paired with a dialkylimidazolium cation and photopolymerized with a comonomer, poly(ethylene glycol) diacrylate (PEGDA), to yield a hierarchically structured copolymer.[16] The copolymer, however, undergoes cation exchange in protic solvents and therefore exhibits poor long-term nanostructure stability.[16] Given these two limitations—lack of mechanical durability and long-term structural integrity—alternative approaches for the preparation of poly(IL)s are needed. Either polymerizing both the IL cation and anion or blending the poly(IL)s with other polymer components may offer a means by which to overcome these limitations. Several recent reports have described the formation of IPNs employing ionic liquid monomers.[17,18] The ionic liquid monomers have been combined with both natural and synthetic polymers to form the IPNs.[17−19] IPNs formed from ionic liquid monomers, however, remain a relatively unexplored area but may offer significant opportunities for producing composite materials with improved materials characteristics or ones that exhibit emergent properties. Herein, we describe a synthetic approach for the preparation of an ionic-liquid-based interpenetrating polymer network (IPN) by sequential photopolymerization of the IL cation followed by the anion to generate a nanostructured and mechanically durable hydrogel.

## EXPERIMENTAL SECTION

**Materials and Methods.** Silver acrylate was purchased from Gelest (Morrisville, PA), and Darocur 1173 was received as a gift from

**Received:** September 24, 2010
**Revised:** January 18, 2011
**Published:** February 21, 2011

Ciba Chemicals (Tarrytown, NY). All other reagents were used as received from Sigma-Aldrich (Milwaukee, WI). Water used in all experiments was of nanopure quality, 18 MΩ·cm.

**Monomer Synthesis.** Synthesis of the monomer (1-(10-(acryloyloxy)decyl)-3-methylimidazolium chloride), [$AcrC_{10}mim^+$][$Cl^-$] (**1**), was performed in two steps as previously described.[6] First, 10-chlorodecyl acrylate was synthesized by adding a solution of 10-chlorodecanol (10 g, 51.9 mmol) and acryloyl chloride (5.63 g, 62.3 mmol) in acetonitrile (250 mL) and triethylamine (8.7 mL, 62.3 mmol) at 0 °C over a period of 20 min. The reaction mixture was then allowed to warm to room temperature and stirred for 24 h. The resulting precipitate was removed by filtration, and volatiles were removed in vacuo. The residue was quenched with dilute hydrochloric acid (1 N, 200 mL) and the crude product extracted from the mixture with ethyl acetate (3 × 100 mL). The organic layers were combined and dried (sodium sulfate), and residual volatiles were removed to obtain a clear yellow oil (11.4 g, 89%).

The 10-chlorodecyl acrylate (11.4 g, 46.4 mmol) and 1-methylimidazole (19.0 g, 231.8 mmol) were heated to 85 °C and stirred for 24 h. The reaction was cooled and the mixture washed with ethyl acetate (3 × 50 mL) to remove any remaining starting material. The crude residue, a mixture of the title compound and polymerized side product, was reduced in vacuo and purified via silica gel column chromatography (20% methanol in acetonitrile). The purified product was taken up in acetonitrile and separated from the silica by filtration to remove any coeluted silica in the final purified product. Volatiles were removed in vacuo to yield a waxy white solid (4.02 g, 26%). $^1$H NMR (500 MHz, $CDCl_3$) $\delta$ (ppm): 11.16 (s, 1H), 7.18 (s, 1H), 7.16 (s, 1H), 6.41−6.38 (dd, $J$ = 17.5 Hz, 1H), 6.15−6.09 (dd, $J$ = 10.0 Hz, 1H), 5.83−5.81 (dd, $J$ = 10.5 Hz, 1H), 4.33−4.30 (t, $J$ = 7.5 Hz, 2H), 4.16−4.13 (t, $J$ = 7.5 Hz, 2H), 4.13 (s, 3H), 1.93−1.90 (m, 2H), 1.68−1.64 (m, 2H), 1.34−1.28 (m, 12H). ATR/FT-IR: 3437, 3392, 3092, 3054, 2925, 2854, 1713, 1633, 1565, 1472, 1411, 1387, 1276, 1196, 1164, 1069, 1038, 1002, 971, 893, 862, 818, 778 $cm^{-1}$.

**Polymer Synthesis.** Poly(1-(10-(acryloyloxy)decyl)-3-methylimidazolium) chloride, poly[$AcrC_{10}mim^+$][$Cl^-$] (**2**), was prepared using the procedure previously described.[14] In a vial, 20 $\mu$L of water was added to 1-(10-(acryloyloxy)decyl)-3-methylimidazolium chloride (**1**) (100 mg). The initial water content of the starting monomer was 5 ± 1% w/w (as determined by TGA), making the total calculated aqueous content 21 ± 3% w/w. The vial was capped tightly and vortex mixed until homogeneous. The mixture was loaded into a borosilicate glass pipet using negative pressure and placed ca. 2−3 in. from a high-intensity UV light source (Hanovia 400 W mercury arc lamp, $\lambda$ = 254 nm) and irradiated for 2 h. The resulting polymer was removed from the pipet by breaking the glass with a razor blade to yield a free-standing pale yellow polymer. ATR/FT-IR: 3370, 3250, 2925, 2854, 1732, 1573, 1467, 1167, 758 $cm^{-1}$.

Poly(1-(10-(acryloyloxy)decyl)-3-methylimidazolium) acrylate, poly[$AcrC_{10}mim^+$][$Acr^-$] (**3**). Poly(1-(10-(acryloyloxy)decyl)-3-methylimidazolium) chloride (**2**) (100 mg, 0.3 mmol) was added to a (2:1) ethanol:water solution (18 mL) of silver acrylate (54 mg, 0.3 mmol) in a 50 mL round-bottom flask under an argon atmosphere at 21 °C for 1 h in the dark. The swollen polymer was filtered and washed in the dark with copious amounts of water and ethanol to remove surface adsorbed silver chloride. ATR/FT-IR: 3442, 3354, 3092, 2928, 2854, 1733, 1635, 1562, 1467, 1412, 1347, 1262, 1167, 993, 947, 838 $cm^{-1}$.

Poly(1-(10-(acryloyloxy)decyl)-3-methylimidazolium)-*inter*-poly(acrylate), poly[$AcrC_{10}mim^+$]-*inter*-poly[$Acr^-$] (**4**). The swollen polymer **3** (8−100 mg, 0.02−0.3 mmol) was placed in a Petri dish and incubated in an aqueous solution (20 mL) of excess Darocur 1173 (20 $\mu$L, 0.13 mmol) for 10 min, permitting the photoinitiator to permeate into the poly(1-(10-(acryloyloxy)decyl)-3-methylimidazolium) acrylate. The polymer was then placed ∼2 in. from a UV light source (UVP 100 W mercury spot lamp, $\lambda$ = 365 nm) for 5 min. ATR/FT-IR: 3383, 2925, 2854, 1732, 1567, 1458, 1375, 1262, 1168 $cm^{-1}$.

**Physical Methods.** Polarized optical microscopy was performed on a Bausch & Lomb Micro Zoom microscope equipped with a custom-made Peltier temperature controller unit. All NMR was performed on a Bruker model DMX 500 NMR spectrometer (11.7 T) equipped with a three-channel, 5 mm inverse detection, three-axis gradient, variable temperature probe with $^2$H lock at 76.773 MHz. ATR/FT-IR spectroscopy was performed using a Bruker Vertex 70 spectrometer over the frequency range 4000−700 $cm^{-1}$ with spectra recorded at 4 $cm^{-1}$ resolution and averaged over 256 scans. Differential scanning calorimetry (DSC) was performed on a Q100 instrument (TA Instruments, New Castle, DE) interfaced with a refrigerated cooling system. Weighed amounts (1−5 mg) of the sample were sealed in aluminum pans, and data were collected between −65 and 100 °C at a heating rate of 2 °C/min. Instrument calibration was performed using an indium standard. Thermogravimetric analysis (TGA) was carried out on a TA Instruments Q50 by heating a known amount of sample (10−30 mg) in a platinum pan from 20 °C to a final temperature of 500 °C at a rate of 10 °C/min under $N_2$ flow. Differential thermogravimetric (DTG) plots were derived from TG scans using the software supplied by the TA Instruments. ICP-MS studies were carried out with a Perkin-Elmer ELAN DRC-II ICP-MS at the Analytical Chemistry Laboratory (ACL) at Argonne National Laboratory.

Small-angle X-ray scattering (SAXS) measurements were made using the instrument at the undulator beamline 12ID-C (12 keV) at the Advanced Photon Source (APS) at Argonne National Laboratory. The 2-D scattering profiles were recorded using a custom built CCD detector. The detector is composed of 4 CCD chips and features a 175 mm square active area with 1000 × 1000 pixel resolution. The sample-to-detector distance was such as to provide a detecting range for momentum transfer of 0.01 $Å^{-1} < q < 0.45$ $Å^{-1}$. The scattering vector, $q$, was calibrated using a silver behenate standard at $q$ = 1.076 $Å^{-1}$. The 2-D scattering images were azimuthally averaged to produce plots of scattered intensity, $I(q)$, versus scattering vector, $q$, where $q = 4\pi/\lambda(\sin\theta)$. The value of $q$ is proportional to the inverse of the length scale, $Å^{-1}$. Polymer samples were probed by orienting the cylindrical samples with their long axis perpendicular to the incident X-ray beam. All measurements were made at 25 °C (±1 °C).

**Swelling Studies.** Equilibrium swelling studies in a range of solvents was carried out on polymers cut into cylindrical pieces with the dimensions 4.0−6.0 mm × 1.0 mm ($l \times w$). Each piece was fully immersed into one of the following solvents: hexanes (HEX), ethyl acetate (EtOAc), ethylene glycol (EGly), chloroform ($CHCl_3$), acetonitrile (ACN), dimethylformamide (DMF), ethanol (EtOH), methanol (MeOH), and water. After 24 h the samples were removed from the solvent, placed on a paper towel to remove excess solvent, and their length and width measured. Sample volume was calculated to obtain a ratio of the volume ($V_f$) versus the initial volume ($V_0$) of each sample ($V_f/V_0$). All measurements were made under ambient laboratory conditions: 21 °C (±1 °C), 53% (±3%) relative humidity.

## RESULTS AND DISCUSSION

An ionic liquid interpenetrating polymer network (IPN) is prepared by photopolymerization of the IL cation followed by the introduction and photoirradiation of the anion to form a mechanically durable hydrogel (Figure 1). The starting monomer, (1-(10-(acryloyloxy)decyl)-3-methylimidazolium chloride), [$AcrC_{10}mim^+$][$Cl^-$] (**1**), was synthesized as previously described.[14] The amphiphilic monomer is preassembled into a liquid-crystalline mesophase by the addition of water to yield a total water content of 23 ± 3% (w/w). The mixture is a transparent, homogeneous, and a slightly viscous liquid which, as previously determined by small-angle X-ray scattering (SAXS), adopts a 2-D hexagonal structure possessing some residual

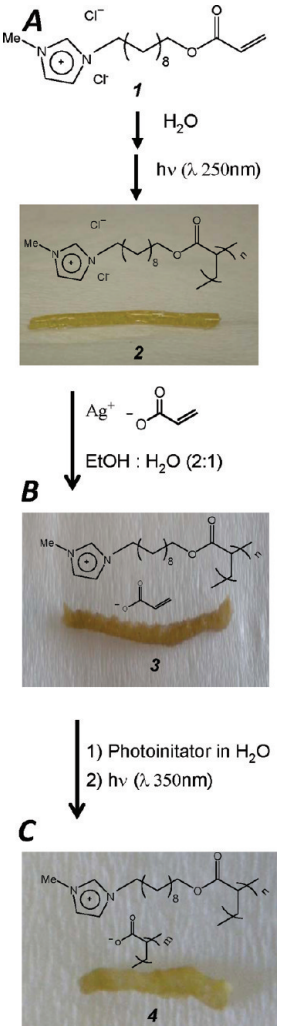


**Figure 1.** Synthetic scheme for preparation of the interpenetrating poly(IL network, poly[$AcrC_{10}mim^+$]-*inter*-poly[$Acr^-$]. (A) [$AcrC_{10}mim^+$][$Cl^-$] (**1**) monomer is self-assembled in 23% (w/w) water and photoirradiated with 254 nm UV light (2 h) to produce poly[$AcrC_{10}mim^+$][$Cl^-$] (**2**). (B) Poly[$AcrC_{10}mim^+$][$Cl^-$] is then anion exchanged with silver acrylate, thereby introducing the acrylate monomer to yield poly[$AcrC_{10}mim^+$]-[$Acr^-$] (**3**). (C) Poly[$AcrC_{10}mim^+$][$Acr^-$] is infused with a photoinitiator (Darocur 1173) and photoirradiated briefly with 365 nm UV light (5 min) to polymerize the acrylate, producing poly[$AcrC_{10}mim^+$]-*inter*-poly[$Acr^-$] (**4**).

tetragonal perforated lamellar (TPL) character.[14] It has been previously noted that the TPL structure is fully formed at lower water contents (5−16% (w/w)).[14] Furthermore, the structural evolution from TPL to 2-D hexagonal structure is consistent with the established structural progression for rod−coil self-assembled systems.[20] Photoinitiated polymerization of the binary mixture by UV irradiation ($\lambda$ = 254 nm for 1.5−2 h) produces a free-standing and elastic cylindrical rod upon release from the borosilicate pipet (Figure 1A).[14] As previously observed, the change in solution consistency to a rubbery solid suggests polymerization of the IL cation, [$AcrC_{10}mim^+$], to form poly[$AcrC_{10}mim^+$][$Cl^-$] (**2**).[14] The successful polymerization of the acryloyl group is confirmed by ATR/FT-IR spectroscopy (Figure 2). The disappearance of the acryloyl $\nu$(−C═C−) stretch at 1633 $cm^{-1}$ is a signature band frequently used to monitor the success or extent of polymerization.[21] Comparison of the spectrum recorded on the

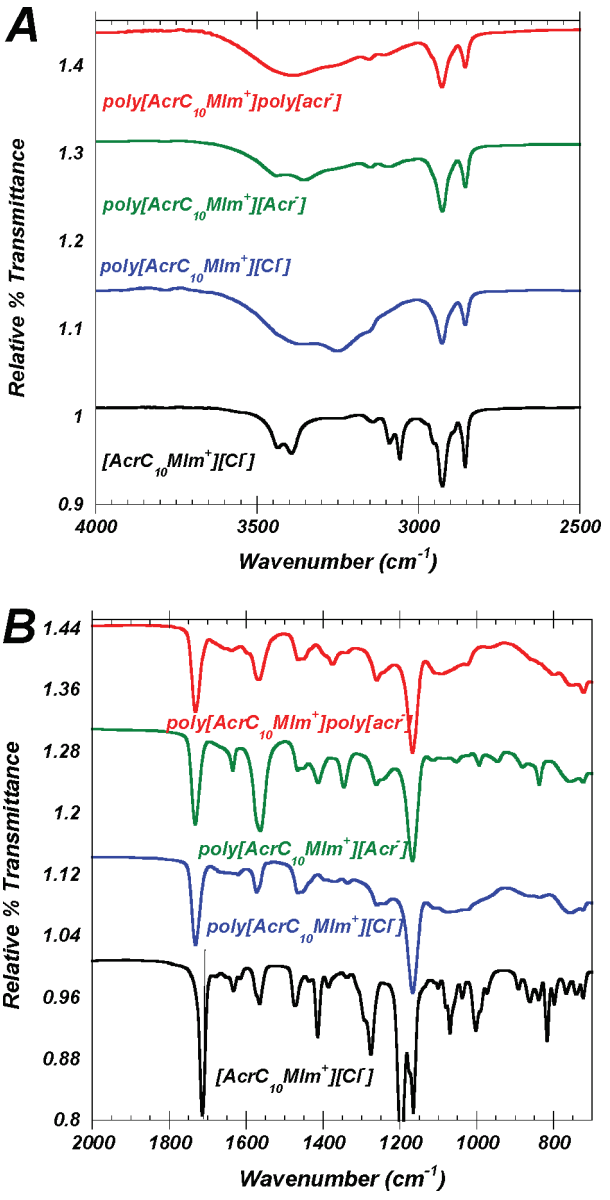


**Figure 2.** ATR/FT-IR spectra of [$AcrC_{10}mim^+$][$Cl^-$] monomer (black), poly[$AcrC_{10}mim^+$][$Cl^-$] (blue), poly[$AcrC_{10}mim^+$][$Acr^-$] (green), and poly[$AcrC_{10}mim^+$]-*inter*-poly[$Acr^-$] (red). (A) 4000−2500 $cm^{-1}$ region; (B) 2000−750 $cm^{-1}$ region.

monomer (**1**) to poly[$AcrC_{10}mim^+$][$Cl^-$] (**2**) shows complete loss of the 1633 $cm^{-1}$ vibrational mode, confirming that polymerization has proceeded to completion. A shift in the acryloyl carbonyl band position at 1713 $cm^{-1}$ to the expected unconjugated mode position at 1732 $cm^{-1}$ is also observed.[21] The loss of several other acryloyl bands, including the $=CH_2$ deformation mode at 1411 $cm^{-1}$, and the =CH and $=CH_2$ rocking modes at 1276 and 1069 $cm^{-1}$, respectively, further confirm polymerization.[13] Successful polymerization is also indicated by the loss of the vinyl C−H bending (1002, 971, 818 $cm^{-1}$) and stretching (3092, 3054 $cm^{-1}$) modes. The 3437 $cm^{-1}$ band, assigned to the $\nu$(O−H) vibrational mode of the acryloyl, is also observed to diminish post-UV-irradiation.[22] Changes in hydrogen-bonding interactions postpolymerization can also be monitored by IR spectroscopy. The broad band centered at 3370 $cm^{-1}$ reflects a distribution of self-associated hydroxyl groups produced upon


dx.doi.org/10.1021/ma102146r |*Macromolecules* 2011, 44, 1421–1428

polymerization.[23] The shift of this band from 3392 $cm^{-1}$ (monomeric form) to 3370 $cm^{-1}$ postpolymerization suggests that intermolecular hydrogen-bonding interactions are strengthened.[23]

In the next step, a polymerizable anion is introduced by anion exchange of the solid, solvent-swollen poly[$AcrC_{10}mim^+$][$Cl^-$] with silver acrylate (Figure 1B). The metathesis reaction is carried out in a 2:1 mixture of ethanol:water to reduce the degree of swelling of poly[$AcrC_{10}mim^+$][$Cl^-$], which is maximally swollen in water and produces a hydrogel with diminished mechanical integrity (Figure S1). The anion-exchange process can be visually monitored by the appearance of a white precipitate (AgCl) in solution within 60 min. The polymer is then removed from solution and washed with copious amounts of ethanol and water. ICP-MS analyses on washed polymers indicate $Ag^+$ remains trapped within the polymer (1.58 ± 0.1 mg of silver/g of polymer). It is noted that prolonged reaction times (>3 h) result in tenacious surface adsorption of AgCl on the exterior surface of the polymer which could not be removed. Successful anion exchange and formation of poly[$AcrC_{10}mim^+$][$Acr^-$] (**3**) was confirmed by ATR/FT-IR (Figure 2) by the reappearance of the acrylate modes, including the acrylate C═C mode at 1635 $cm^{-1}$ and the $\delta(=CH_2)$ mode at 1412 $cm^{-1}$. Also noted is the re-emergence of the vinyl C−H bending modes (993, 947, and 838 $cm^{-1}$) and the acrylate OH vibrational band at 3442 $cm^{-1}$. It is noted that the metathesis reaction does not afford complete exchange of the chloride for the acrylate anion. The extent of exchange is limited by the solubility product of AgCl.[24] $^1$H NMR spectroscopy estimated the extent of anion exchange and was determined to be 80 ± 10%. The experimental procedure does, however, allow for sufficient pairing of the acrylate anion with the polycationic IL in order to proceed with the second step polymerization.

In the final step, poly[$AcrC_{10}mim^+$][$Acr^-$] is swollen in an aqueous solution of a photoinitiator, Darocur 1173, for 10 min, to allow for permeation throughout the network. The initiator-treated poly[$AcrC_{10}mim^+$][$Acr^-$] was then briefly UV irradiated ($\lambda$ = 365 nm, 5 min) to trigger the polymerization and cross-linking through the acrylate counteranion (Figure 1C). The physical appearance of the postirradiated product does not change dramatically from the precursor polymer (Figure 1B). Successful covalent coupling of the acrylate anion in the formation of poly[$AcrC_{10}mim^+$]-*inter*-poly[$Acr^-$] (**4**) is confirmed by ATR/FT-IR (Figure 2). Specifically, disappearance of the acrylate modes at 3442, 1635, 1412, 993, 882, and 838 $cm^{-1}$ confirms successful polymerization. The emergence of a C−H alkane rocking mode at 1375 $cm^{-1}$ suggests cross-linking of the anion groups by formation of alkane chains.[25] Studies employing extended UV-irradiation times (45 min) did not reveal any significant changes in the IR spectrum. Finally, it is noted that all attempts to prepare the polymer directly from the [$AcrC_{10}MIm^+$][$Acr^-$] monomer were not successful, resulting in a nondurable (non-self-supporting) product (liquid) rather than a self-supporting gel.

**Thermal Properties.** The thermal properties of poly-[$AcrC_{10}mim^+$]-*inter*-poly[$Acr^-$] as determined by thermogravimetric analysis (TGA) and differential scanning calorimetry (DSC) are presented in Figure 3. The TGA carried out employing fast scan (10 °C/min) studies under nitrogen shows a multiple-step weight loss profile (Figure 3A). The first region of weight loss (∼10 wt %) occurs up to ca. 150 °C, reflecting removal of residual water from the IPN. The next (main)

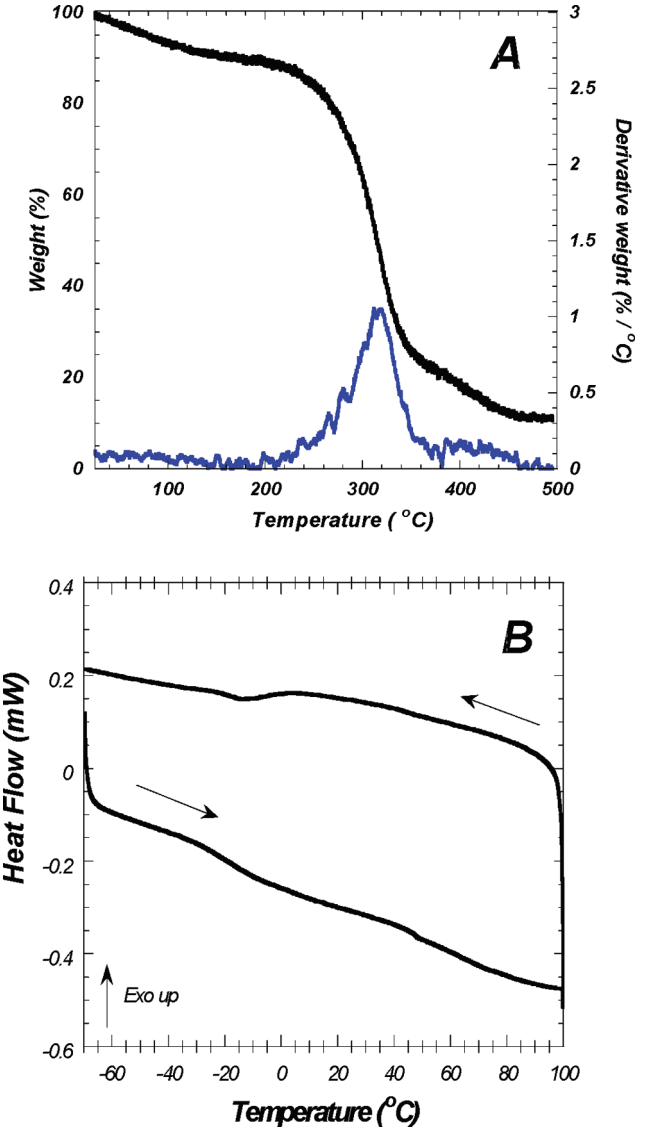


**Figure 3.** (A) Fast scan (10 °C/min), nitrogen atmosphere TGA collected on poly-[$AcrC_{10}mim^+$]-*inter*-poly[$Acr^-$]: weight % (black) and derivative weight loss, DTG (blue). (B) DSC heating and cooling scans (2 °C/min) collected on dried, solid poly[$AcrC_{10}mim^+$]-*inter*-poly[$Acr^-$].

transition occurs at 283 °C (onset; $T_{midpoint}$ = 317 °C). Decomposition to volatile products is incomplete up to 500 °C, with 9 wt % of the sample remaining. The midpoint of the main decomposition transition ($T_d$) is, as expected, higher than that determined for the monomer, [$AcrC_{10}mim^+$][$Cl^-$], which possess a $T_d$ at 287 °C (Figure S2A). It is further noted that the midpoint transition for the monomer ([$AcrC_{10}mim^+$][$Cl^-$]) is ca. 10 °C higher than that previously determined for [$AcrC_8mim^+$][$Cl^-$] ($T_{midpoint}$ = 277 °C).[13] The observed increase is consistent with the insertion of two additional carbons in the alkyl chain.[26] Polymerization of the [$AcrC_{10}mim^+$][$Cl^-$] monomer to yield poly[$AcrC_{10}mim^+$][$Cl^-$] produced a material with a $T_d$ at 306 °C (Figure S2B), which is 24 °C higher than that for the corresponding poly[$AcrC_8mim^+$][$Cl^-$].[13] The $T_d$ determined for poly[$AcrC_{10}mim^+$][$Acr^-$] (Figure S2C) is 312 °C. The observed increase in $T_d$ most likely arises from thermally triggered cross-linking/oligomerization induced upon heating. The second

polymerization step that produces the IPN, poly[AcrC$_{10}$mim$^+$]-*inter*-poly[Acr$^-$], results in a 11 °C ($T_{midpoint}$ = 317 °C, Figure 3A) increase in the $T_d$ compared to the poly[AcrC$_{10}$mim$^+$][Cl$^-$]. Such a modest increase in the $T_d$ is not uncommon for polymer blends, and a decrease in the $T_d$ has even been previously reported. The decrease in $T_d$ was attributed to unfavorable interactions arising between functional groups upon interpenetration of two different polymers.[27,28] For example, it has been reported that pseudo-hydrogen bonding between C−H groups on poly(vinylidene fluoride) (PVDF) and the C═O groups on poly(vinylpyrrolidone) (PVP) catalyzes the thermal decomposition of PVDF/PVP composites.[27] Therefore, the slight observed increase in $T_d$ of poly[AcrC$_{10}$mim$^+$]-*inter*-poly[Acr$^-$] instead of a decrease may reflect the inherent compatibility of the two acrylate polymers. Moreover, the interaction between the two polymers in the IPN is most likely due to physical cross-links since chemical cross-links are expected to cause a greater increase in the $T_d$. For example, a very high thermal decomposition temperature was determined for *net*-poly[C$_{10}$mim$^+$][Acr$^-$]-*co*-PEGDA ($T_{midpoint}$ = 408 °C), most likely due to the formation of an extensive chemically cross-linked network.[16]

The DSC thermogram (Figure 3B) collected on poly-[AcrC$_{10}$mim$^+$]-*inter*-poly[Acr$^-$] is devoid of any first-order phase transitions over the experimental range studied, −70 → 100 °C (a maximum temperature well below the determined onset of thermal decomposition). A weak secondary phase transition, $T_g$, is observed in the second heating scan with a midpoint positioned at −16.1 ± 10 °C and is reversible upon cooling (Figure 3B). A single $T_g$ suggests a well-mixed blend of the two polymers (i.e., lack of phase separation) in the formed IPN.[29,30] The observed $T_g$ is higher than that of both poly-[AcrC$_{10}$mim$^+$][Cl$^-$] ($T_g$ midpoint transition at −40.6 ± 5 °C; Figure S2D) and poly[AcrC$_{10}$mim$^+$][Acr$^-$] ($T_g$ midpoint transition at −33.12 ± 5 °C; Figure S2E). An increased $T_g$ with IPN formation may signal the presence of hydrogen bonds between the two component polymers.[31] That is, the increased $T_g$ arises from the interlocked (i.e., hydrogen bonded) network which acts to reduce molecular mobility but also serves to diminish phase separation.[32] Strong hydrogen bonds can form, for example, between the carbonyl group of a methyl acrylate and a dialkylimidazolium cation.[33] It is further noted that the temperature interval over which the $T_g$ occurs for the IPN is broader than for the precursor polymers either due to heterogeneities on the nanoscale or a distribution of $T_g$ values.[34] Lastly, in addition to the $T_g$, a small endothermic phase transition is observed at ∼47 °C in the DSC heating scan (Figure 3B). This phase transition arises from the liquid-crystalline to isotropic state conversion as evidenced by loss of the optical birefringence when observed under polarized light.

**Mesoscale Structure.** The poly[AcrC$_{10}$mim$^+$][Cl$^-$] is liquid crystalline as evidenced by optical birefringence observed when examined under polarized light (Figure 4A). Also, noted is a disordered herringbone structured wrinkle pattern (Figure 4A) that may have been generated upon solvent contact (partial swelling) and extraction of the polymer from the capillary postpolymerization.[35] Under high magnification, regions are identified with optical textures characteristic of a columnar phase (Figure 4A, inset). The X-ray scattering studies carried out on poly[AcrC$_{10}$mim$^+$][Cl$^-$] yielded a diffraction pattern (Figure 4B) possessing three resolvable peaks at $q$ = 0.195, 0.339, 0.394 Å$^{-1}$ ($\sqrt{1}$, $\sqrt{3}$, $\sqrt{4}$) which index to a 2-D hexagonal structure (Figure 4J) with a $d$-spacing of 32.2 Å and an intercolumnar center-to-center distance of 37.2 Å. The pattern agrees well with that reported for poly[AcrC$_{10}$mim$^+$][Cl$^-$] prepared from intermediate water content in the binary mixture (20−25% (w/w)).[14] The intensity pattern of the averaged data (Figure 4B) and textures (along the meridional axis) in the 2-D SAXS pattern (Figure 4C) have been previously determined to arise from the presence of a residual tetragonal perforated lamellar (TPL) structure formed at lower water contents (Figure 4K).[14] The TPL structure is intermediate between a lamellar and columnar phase. The symmetry of this morphology is distinguished from a conventional lamellar structure in that the sheets possess in-plane perforations centered at tetragonally distorted bcc positions. The coexistence of a tetragonal perforated lamellar and a 2-D hexagonal structure is consistent with the established structural progression for rod−coil self-assembled systems.[20] Anion exchange of the chloride for acrylate to form the single network polymer poly[AcrC$_{10}$mim$^+$][Acr$^-$] results in the loss of regions of fanlike textures in the polarized optical micrograph (Figure 4D), suggesting a reduction in columnar structure.[36] The scattering pattern (Figure 4E) also displays three diffraction peaks indexed to a 2-D hexagonal structure ($q$ = 0.189, 0.328, 0.379 Å$^{-1}$) with a slight $d$-spacing increase to 33.2 Å consistent with insertion of a bulkier anion (acrylate for chloride). The intensity pattern in the averaged data and the textures in the 2-D image (Figure 4F) again suggest the presence of a residual TPL component. Photopolymerization of the acrylate counteranion to yield the IPN results in further changes in both the optical birefringence (Figure 4G) and the X-ray scattering data (Figure 4H,I). Specifically, the optical textures become more smectic in character, suggesting formation of a lamellar structure and loss of the columnar phase. The averaged SAXS data (Figure 4H) show two Bragg peaks positioned at $q$ = 0.190 and 0.379 Å$^{-1}$ which are indexed to a lamellar structure with a repeat distance of 33.0 Å. The persistence of the intensity pattern and textures in the 2-D image again suggest residual TPL character in the IPN. Thus, each polymerization step results in phase symmetry reduction as previously observed.[13,14,37]

**Solvent Interactions.** The IPN maximally swells in water and short chain alcohols (e.g., methanol or ethanol) to produce a colorless, optically transparent self-supporting gel (Figure 5). In contrast, poorly swollen polymers result from incubation in hexane, ethyl acetate, chloroform, or acetonitrile. More complete examination of the swelling characteristics of the polymer was carried out by determining the equilibrium volume swelling ratio ($V_f/V_o$ at $t$ = 24 h) in solvents selected over a wide range of (Hansen) solubility parameters (Figure 5B). As shown in Figure 5B, maximum polymer swelling (ca. 60 times its original volume) is observed in water, with a $\delta$ value of 48 MPa$^{1/2}$ (23.5 cal$^{1/2}$ cm$^{-3/2}$). Because the degree of swelling is maximized for the polymer network in solvents with similar solubility parameters (i.e., cohesive interactions), the measured value in water provides a good estimation for the IPNs solubility parameter.[13,38] The plot in Figure 5B indicates that, in general, with increasing polarity, the polymer solubility increases. Among the organic solvents examined, polar organics (e.g., short-chain alcohols, ethylene glycol) produce well-swollen polymers, while nonpolar solvents such as hexane yield minimally swollen materials. The solubility characteristics of the IPN compare favorably with the Hildebrand solubility parameters determined for 1-alkyl-3-methylimidazolium-based ionic liquids.[39] Prior work has

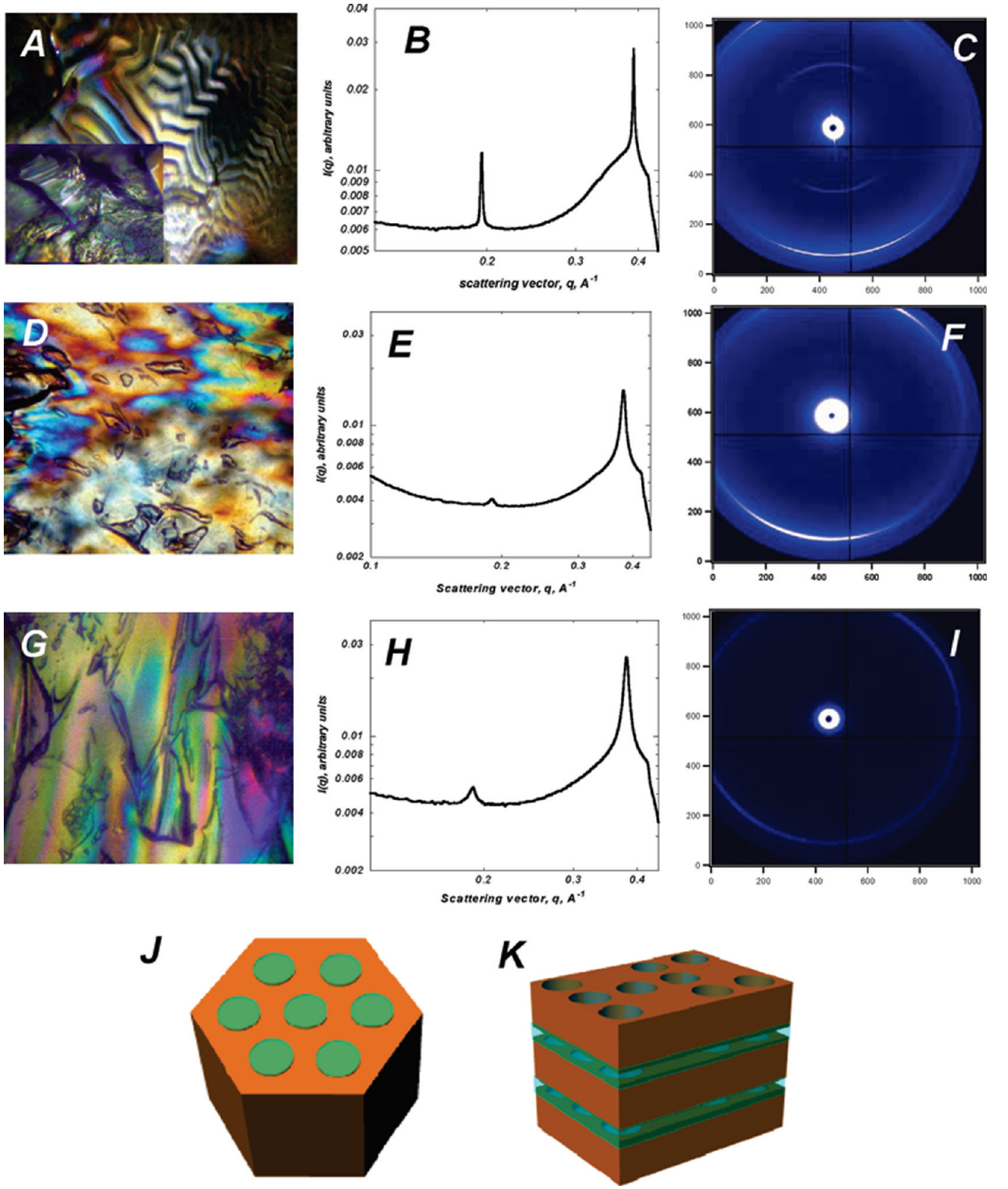


**Figure 4.** (A) Representative polarized optical micrograph, (B) small-angle X-ray scattering (SAXS) azimuthally averaged data, and (C) SAXS 2-D pattern collected on deswollen poly-[AcrC$_{10}$mim$^+$][Cl$^-$]. (D) Representative polarized optical micrograph, (E) SAXS azimuthally averaged data, and (F) 2-D pattern collected on deswollen poly[AcrC$_{10}$mim$^+$][Acr$^-$]. (G) Representative polarized optical micrograph, (H) SAXS azimuthally averaged data, and (I) SAXS 2-D pattern collected on deswollen poly[AcrC$_{10}$mim$^+$]-*inter*-poly[Acr$^-$]. (J) Schematic illustration of a 2-D hexagonal structure. (K) Schematic illustration of a lamellar structure with some tetragonal perforations in the plane of the sheets.

determined that poly(alkyl)acrylate solubility parameters are typically in the range of 16−25 MPa$^{1/2}$, showing miscibility with weakly polar, hydrogen-bonding solvents.[40] The observed swelling of the IPN in polar, hydrogen-bonding

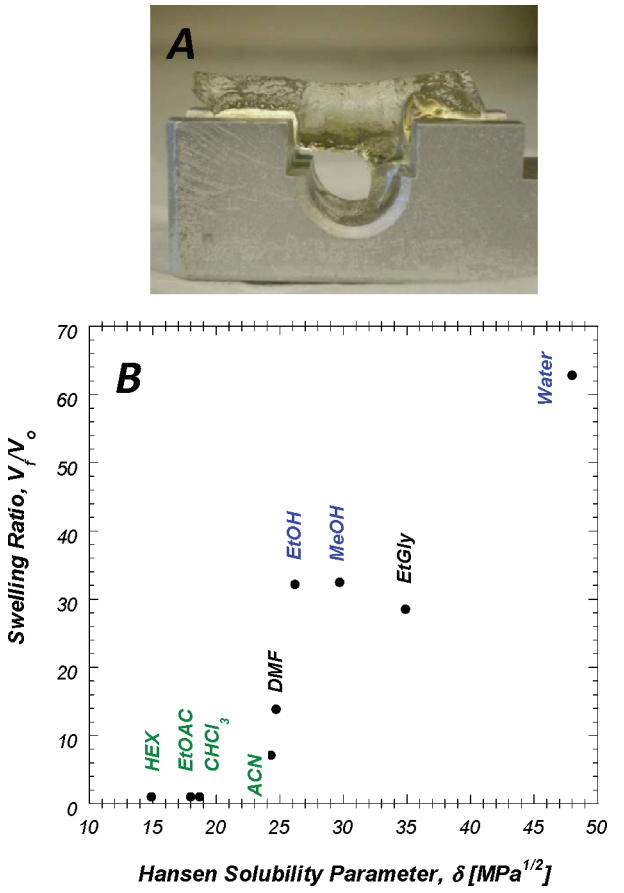


**Figure 5.** (A) Photograph of fully ethanol swollen poly-[$AcrC_{10}mim^+$]-*inter*-poly[$Acr^-$]. (B) Equilibrium volume changes ($V_f/V_o$) of poly-[$AcrC_{10}mim^+$]-*inter*-poly[$Acr^-$] as a function of Hansen solubility parameter evaluated for a range of organic solvents and water after 24 h of incubation.

solvents (solubility parameters in the range of 25−45 MPa$^{1/2}$) must therefore arise from preferential solvation of the imidazolium headgroup rather than poly(alkyl)acrylate backbone. Comparison of the swelling characteristics of poly[$AcrC_{10}mim^+$][$Cl^-$] and poly[$AcrC_{10}mim^+$][$Acr^-$] reveals that IPN formation serves to reduce the swelling behavior in polar organics (Figure S1). Thus, incorporation of the poly(acrylate) network and hydrogen-bonding interactions between the two network polymers serves to decrease the swelling ratio.[41]

## CONCLUSIONS

A sequential IPN has been prepared by photopolymerization of a self-assembled binary mixture of a dialkylimidazolium cation and water followed by introduction and photopolymerization of the IL anion. According to both optical microscopy and X-ray scattering, the synthetic pathway permits retention of liquid crystallinity. The structure, as determined by SAXS, is lamellar with some residual in-plane tetragonally ordered aqueous pores (Figure 4K). The IPN is interlaced and physically cross-linked as suggested by the inability to dissolve the blend in a wide variety of organic solvents or water. DSC, a widely used technique for the study of miscibility and phase separation in multicomponent polymeric systems, reveals a single glass transition. Thus, based upon the thermal analysis studies, the two component polymers, poly[$AcrC_{10}mim^+$] and poly[$Acr^-$], are chemically compatible (miscible), producing a single phase full-IPN. Successful polymer chain interpenetration results in enhanced dimensional stability not observed in the precursor homopolymers. It is further noted that the improved mechanical strength of the solvent swollen IPN is achieved. The improvement in mechanical strength is achieved while maintaining some level of environmental responsiveness (swell and deswell). The hierarchical structure generated offers the possibility of sequestering both lipophilic and water-soluble guests into the IPN, and the sequential polymerization approach offers a potentially benign route for the introduction and stable encapsulation of guest molecules. Future studies will be directed at examining the use of the IPN hydrogel for the stable encapsulation of both membrane and water-soluble proteins. More importantly, the modularity of the synthetic approach offers additional opportunities for the incorporation of functionality into the material, possibly allowing for matrix control or activation of encapsulated guests.

## ASSOCIATED CONTENT

**Supporting Information.** Thermograms and solvent studies for both poly[$AcrC_{10}mim^+$][$Cl^-$] and poly[$AcrC_{10}mim^+$]-[$Acr^-$]. This material is available free of charge via the Internet at http://pubs.acs.org.

## AUTHOR INFORMATION

### Corresponding Author

*Phone 630-252-8298; Fax 630-252-9151; e-mail firestone@anl.gov.

## ACKNOWLEDGMENT

We acknowledge Dr. Sungwon Lee for rendering the POV ray images. This work was performed under the auspices of the Office of Basic Energy Sciences, Division of Materials Sciences, United States Department of Energy, under Contract No. DE-AC02-06CH1135.

## REFERENCES

(1) Sperling, L. H.; Fay, J. J.; Murphy, C. J.; Thomas, D. A. *Makromol. Chem., Macromol. Symp.* **1990**, *38*, 99–113.
(2) Sperling, L. H.; Mishra, V. *Polym. Adv. Technol.* **1996**, *7*, 197–208.
(3) Ohno, H. *Bull. Chem. Soc. Jpn.* **2006**, *79*, 1665–1680.
(4) Green, O.; Grubjesic, S.; Lee, S.; Firestone, M. A. *Polym. Rev.* **2009**, *49*, 339–360.
(5) Green, M. D.; Long, T. E. *Polym. Rev.* **2009**, *49*, 291–314.
(6) Lu, J.; Yan, F.; Texter, J. *Prog. Polym. Sci.* **2009**, *34*, 431–448.
(7) Yazaki, S.; Funahashi, M.; Kagimoto, J.; Ohno, H.; Kato, T. *J. Am. Chem. Soc.* **2010**, *132*, 7702–7708.
(8) Lee, M.; Choi, H.; Colby, R. H.; Gibson, H. W. *Chem. Mater.* **2010**, *22*, 5814–5822.
(9) Marcilla, R.; Mecerreyes, D.; Winroth, G.; Brovelli, S.; Yebra, M. D. R.; Cacialli, F. *Appl. Phys. Lett.* **2010**.
(10) Zhao, Q. C.; Wajert, J. C.; Anderson, J. L. *Anal. Chem.* **2010**, *82*, 707–713.
(11) Yoshio, M.; Kagata, T.; Hoshino, K.; Mukai, T.; Ohno, H.; Kato, T. *J. Am. Chem. Soc.* **2006**, *128*, 5570–5577.

(12) Yoshizawa, H.; Mihara, T.; Koide, N. *Liq. Cryst.* **2005**, *32*, 143–149.
(13) Batra, D.; Hay, D. N. T.; Firestone, M. A. *Chem. Mater.* **2007**, *19*, 4423–4431.
(14) Batra, D.; Seifert, S.; Firestone, M. A. *Macromol. Chem. Phys.* **2007**, *208*, 1416–1427.
(15) Ohno, H.; Yoshizawa, M.; Ogihara, W. *Electrochim. Acta* **2004**, *50*, 255–261.
(16) Grubjesic, S.; Seifert, S.; Firestone, M. A. *Macromolecules* **2009**, *42*, 5461–5470.
(17) Vidal, F. D. R.; Juger, J.; Chevrot, C.; Teyssi, D. *Polym. Bull.* **2006**, *57*, 473–480.
(18) Kadokawa, J. I.; Murakami, M.-a.; Kaneko, Y. *Compos. Sci. Technol.* **2008**, *68*, 493–498.
(19) Prasad, K.; Kadokawa, J. *Polym. Compos.* **2010**, *31*, 799–806.
(20) Ryu, J.-H.; Oh, N.-K.; Zin, W.-C.; Lee, M. *J. Am. Chem. Soc.* **2004**, *126*, 3551–3558.
(21) Wall, B. G.; Koenig, J. L. *Appl. Spectrosc.* **1997**, *51*, 1453–1459.
(22) Zhong, B.; Chen, D. B.; Zhou, Z. H. *J. Appl. Polym. Sci.* **1998**, *69*, 1599–1606.
(23) Liu, Y.; Goh, S. H.; Lee, S. Y.; Huan, C. H. A. *Macromolecules* **1999**, *32*, 1967–1971.
(24) Firestone, M. A.; Rickert, P. G.; Seifert, S.; Dietz, M. L. *Inorg. Chim. Acta* **2004**, *357*, 3991–3998.
(25) Wang, R. W.; Baran, G.; Wunder, S. L. *Langmuir* **2000**, *16*, 6298–6305.
(26) Fox, D. M.; Awad, W. H.; Gilman, J. W.; Maupin, P. H.; De Long, H. C.; Trulove, P. C. *Green Chem.* **2003**, *5*, 724–727.
(27) Chen, N.; Hong, L. *Solid State Ionics* **2002**, *146*, 377–385.
(28) Schmiesser, J.; Holdcroft, S.; Yu, J.; Ngo, T.; McLean, G. *Chem. Mater.* **2005**, *17*, 387–394.
(29) Tamai, T.; Imagawa, A.; Trancong, Q. *Macromolecules* **1994**, *27*, 7486–7489.
(30) Yang, Z.; Han, C. D. *Macromolecules* **2008**, *41*, 2104–2118.
(31) Tan, Y. Z.; Xu, M. C.; Li, H. T. *Chin. Chem. Lett.* **2005**, *61*, 1597–1599.
(32) Jiang, M.; Xiao, H.; Jin, X. L.; Yu, T. Y. *Polym. Bull.* **1990**, *23*, 103–109.
(33) Welton, T. *Coord. Chem. Rev.* **2004**, *248*, 2459–2477.
(34) Duenas, J. M. M.; Escuriola, D. T.; Ferrer, G. G.; Pradas, M. M.; Ribelles, J. L. G.; Pissis, P.; Kyritsis, A. *Macromolecules* **2001**, *34*, 5525–5534.
(35) Yang, S. I.; Khare, K.; Lin, P.-C. *Adv. Funct. Mater.* **2010**, *20*, 2550–2564.
(36) Chuang, W. T.; Sheu, H. S.; Jeng, U. S.; Wu, H. H.; Hong, P. D.; Lee, J. *Chem. Mater.* **2009**, *21*, 975–978.
(37) Batra, D.; Seifert, S.; Varela, L. M.; Liu, A. C. Y.; Firestone, M. A. *Adv. Funct. Mater.* **2007**, *17*, 1279–1287.
(38) Mutelet, F.; Butet, V.; Jaubert, J. N. *Ind. Eng. Chem. Res.* **2005**, *44*, 4120–4127.
(39) Lee, S. H.; Lee, S. B. *Chem. Commun.* **2005**, 3469–3471.
(40) *Polymer Handbook*, 3rd ed.; Brandrup, J., Immergut, E., Eds.; Wiley-Interscience: New York, 1989.
(41) Zhang, J.; Peppas, N. A. *Macromolecules* **2000**, *33*, 102–107.